Available online at www.sciencedirect.com
SCIENCE DIRECT
Thin Solid Films 513 (2006) 114–117
thin solid films
www.elsevier.com/locate/tsf

The growth of single cubic phase ZnS thin films on silica glass by plasma-assisted metalorganic chemical vapor deposition

Z.Z. Zhang, D.Z. Shen *, J.Y. Zhang, C.X. Shan, Y.M. Lu, Y.C. Liu, B.H. Li, D.X. Zhao, B. Yao, X.W. Fan

Key Laboratory of Excited State Processes, Chinese Academy of Sciences, Changchun Institute of Optics, Fine Mechanics and Physics, Chinese Academy of Sciences, 16-Dongnanhu Road, Changchun, 130033, PR China

Received 16 July 2004; received in revised form 21 October 2005; accepted 19 January 2006
Available online 28 February 2006

Abstract

In this work, ZnS thin films with single-phase zinc blende structure were fabricated on silica glass substrates by plasma-assisted metalorganic chemical vapor deposition (PA-MOCVD). Dimethyl zinc and hydrogen sulfide were used as the precursors. The films were characterized using X-ray diffraction and photoluminescence spectroscopy. The optimal temperature for ZnS growth, 350 °C, was confirmed via a series of growth at different temperatures. In order to obtain stoichiometric ZnS films using PA-MOCVD, larger VI/II gas flow ratios was needed than the one used without plasma assistance. The reason for this phenomenon is discussed.

PACS: 68.55Nq; 78.55Et; 81.15Gh
Keywords: Zinc sulphide; Luminescence; Mental organic; Chemical vapor; X-ray diffraction

1. Introduction

ZnS, with a direct wide gap of 3.7 eV [1], has attracted attention in recent years due to its promising applications in short-wavelength light emitting diodes and laser diodes [2]. Many growth techniques have been reported to prepare ZnS thin films, such as sputtering [3], pulsed-laser deposition [4], metal-organic chemical vapor deposition [5–8], molecular beam epitaxy [9], photochemical deposition [10] and chemical bath deposition [11]. In general, ZnS exhibits two stable phases at room temperature, zinc blende phase with cubic structure and wurtzite phase with hexagonal structure, respectively. The difference between the two phase structures lies only in the stacking sequences along the *c*-axis of the hexagonal phase and the (111) axis of the cubic phase. Usually, it is not easy to grow single-phased ZnS films using conventional growth techniques. Single-phased thin films can be fabricated selectively by properly controlling the growth parameters, and choosing substrates with appropriate lattice parameters and polar orientations. Because of the large difference vapor pressure between zinc and sulfur, the ZnS films produced by vapor deposition are usually non-stoichiometric. It is another important issue to control the S/Zn ratio for growth of stoichiometric ZnS thin films. In this paper, we report our successful growth of ZnS thin films with single-phase zinc blende structure on silica glass substrates by using plasma-assisted metalorganic chemical vapor deposition (PA-MOCVD) method. Effect of the plasma assistance on the stoichiometric ratio of the ZnS films was investigated. The large number of ions and electrons in the plasma with high energy benefit the precursors' decomposition, therefore, the growth process is affected significantly by the plasma assistance. The PA-MOCVD growth technique makes it possible to grow high quality ZnS thin films even on non-crystal substrates at a relatively low substrate temperature, which is beneficial for controlling doping and minimizing interface diffusion between films and substrates.

2. Experiment

The PA-MOCVD system is sketched in Fig. 1. The silica glass substrate was placed on the graphite susceptor. The heating

* Corresponding author. Tel.: +86 431 6176322; fax: +86 431 4627031.
E-mail address: zzzhang@jlmc.com.cn (D.Z. Shen).

0040-6090/$ - see front matter © 2006 Elsevier B.V. All rights reserved.
doi:10.1016/j.tsf.2006.01.054

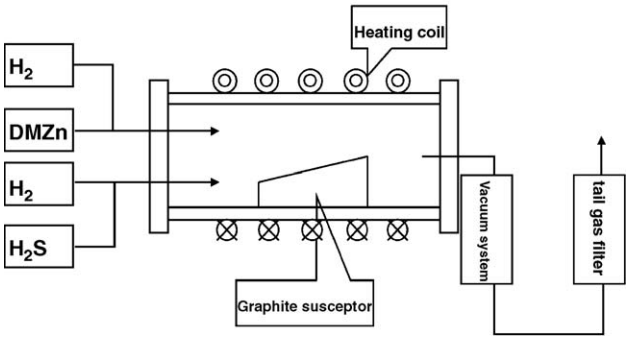

Fig. 1. Sketch of the PA-MOCVD system.

coil acts as the heater for the susceptor via electromagnet induction and also as the plasma generator when the gas pressure in the growth chamber reaches a certain degree. H_2S and dimethyl zinc (DMZn) were used as the precursors. Hydrogen purified by palladium was used as the carrier gas. The flow rates of DMZn and H_2S were 2.85×10^{-5} mol/min and $1.7\sim4\times10^{-4}$ mol/min, respectively. The radio-frequency for the heating coil was 0.5 MHz. The total pressure was kept at about 1000 Pa, and the total H_2 flow rate was 800 standard cubic centimeters per minute. In order to find the optimal temperature for the growth of ZnS thin films with plasma assistance, a series of growth was performed at 100, 150, 250, 300, 350, and 400 °C, respectively. The thickness of the films was all about 1 μm measured via the cross-section image by using scanning electron microscopy (SEM). The structure of the ZnS thin films were characterized by X-ray diffraction (XRD) using an X-ray diffractometer (D/max-RA) with Cu Ka source (0.154 nm). The stoichiometric ratio of S/Zn in the films was measured by energy dispersive X-ray spectrometry in a SEM. A Jobin-Yvon 630 micro spectrometer was employed to measure the photoluminescence (PL) of the samples at room temperature and the excitation source was the 325 nm line of a He–Cd laser.

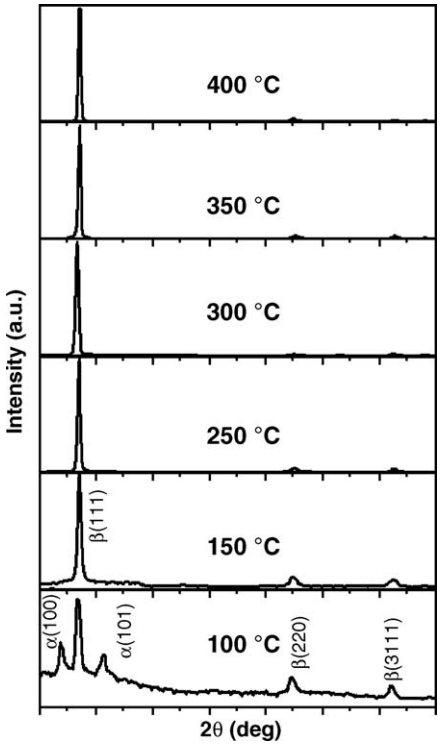

Fig. 2. XRD spectra of the ZnS thin films grown at different temperatures with the plasma assistance. Symbol α and β denote the hexagonal and the cubic phase, respectively.

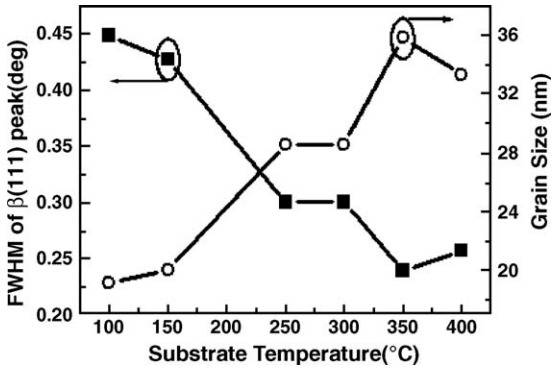

Fig. 3. Growth temperature dependence of the FWHW of β [111] XRD peak and grain size of the ZnS films.

3. Result and discussion

Fig. 2 is the XRD spectra of the ZnS thin films grown at different temperatures with plasma assistance. The evolvement of the XRD spectra with increasing growth temperature is roughly the same as that reported in Ref. [12], in which the ZnS films were grown without plasma assistance. In the spectrum of the sample grown at 100 °C, five diffraction peaks are observed, which are originated from different phases of ZnS. The peaks located at 27.0° and 30.7°, labeled with α[100] and α[101], are due to the [100] and [101] peaks of wurtzite structure. The peaks at 28.4°, 47.3° and 56.1°, labeled with β [111], β [220] and β [311], were attributed to the [111], [220] and [311] diffraction peaks of zinc blende structure. It means that the sample grown at 100 °C is a mixed-crystal of wurtzite (hexagonal) and zinc blende (cubic) phases. As the substrate temperature was increased to 150 °C, the wurtzite peaks disappeared. Meanwhile, the relative intensities of the β [220] and β [311] peaks decreased slightly in comparison with that of the β [111] signal. As the growth temperature increases further, the β [220] and β [311] peaks weakened, implying that the films transformed into single-phased zinc blende structure and tended to grow along the β [111] direction. In general, for a ZnS crystal, the zinc blende structural phase is stable at low temperature and the wurtzite structural phase is stable at temperature higher than 1023 °C [13]. Therefore, the wurtzite phase appeared in the film grown at 100 °C is not thermodynamically stable. Low growth temperature results in the poor mobility of atoms, so some atoms deposited on the surface cannot form the more stable blende phase before the atoms of next layer reach the surface. Considering the significant signal noise in the spectrum of the sample grown at 100 °C, it can be concluded that there also exists non-crystal ZnS in the film besides the wurtzite and blende phases. Fig. 3 depicts the variance of the full width at half maxim (FWHM) of the β [111] peak as a function of increasing substrate

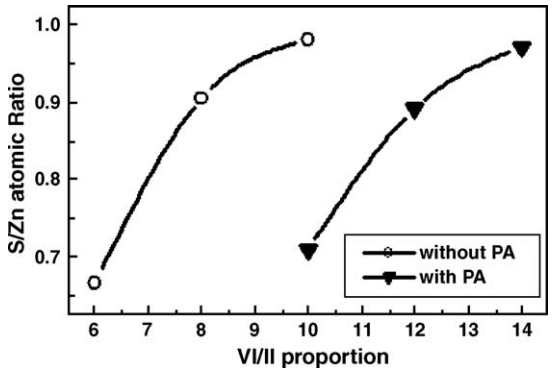

Fig. 4. Relationship between the S/Zn atomic ratio in ZnS films and the VI/II flow proportion.

temperature. As can be seen, the β [111] peak narrows continuously as increase of the substrate temperature. When the substrate temperature increases to 350 °C, the FWHW of β [111] reaches the minimum 0.24 °C. When the substrate temperature is over 400 °C, the FWHW of the β [111] peak increases again. According to Scherrer fomular [14], $d=0.94\lambda/B\cos\theta$, we can calculate the grain size of the samples grown at different temperature, where d is the grain diameter, λ is the wavelength of the X-ray, B is the FWHM of the diffraction peak expressed in radians and θ is the Bragg diffraction angle. As shown in Fig. 3, the grain size increases as the temperature rises, and reaches a maximum of 35.8 nm at 350 °C. During this process, the mobility of the surface atoms is enhanced gradually, making the atoms' transfer to appropriate positions possible. The high atomic mobility is beneficial in enabling the growth of the crystal into a larger grain size. When the growth temperature increases further to 400 °C, the grain size decreases again. High temperature enhances the pre-reactions of the precursors, leading to form more nuclear sites on the substrate. Additionally, desorption of Zn and S atoms at high temperature limits the growth of the crystal grain. These two factors result in the decreasing of the grain size. Analysis based on the XRD spectra indicated that the films grown at 350 °C have the highest crystal quality. Therefore, 350 °C was selected as the optimal temperature for the ZnS thin film growth in this work.

In growth of compound materials that are composed of elements with different vapor pressures, the samples usually deviate from stoichiometric ratio. This problem occurs frequently in ZnS films fabrication. In order to obtain stoichiometric matched ZnS films, we have grown the thin films using different VI/II flow proportions at 350 °C. Fig. 4 shows the relationship between the S/Zn atomic ratio and the VI/II flow rate proportions. The S/Zn atomic ratio increases with increasing the VI/II flow rates proportions. In the case of ZnS growth without plasma assistance, when the VI/II flow rates proportion reaches 10:1, the atomic ratio of S/Zn approximates 1:1. For the ZnS growth with plasma assistance, although the evolvement is similar to the case without plasma assistance, the stoichiometric S/Zn atomic ratio is obtained till the VI/II flow rates proportion reaches 14:1. In the growth process, the precursors adsorb on the substrate surface, and lose the methyl or H atoms followed by forming ZnS. In the case of ZnS growth without plasma assistance, the thermal inducement of the substrate acts as a crucial role in the dissociation process of precursors. However, under the effect of the plasma, high energy is provided to the precursor molecules in vapor phase by colliding with hot electrons so that the molecules have higher chemical activity, which benefits the bonding between the precursors and the film surface. For DMZn, the first $Zn–CH_3$ bond dissociation energy is $E_1=63.7\pm1.5$ kcal/mol, and the second dissociation energy is $E_2=24.5\pm4.0$ Kcal/mol [15]. The S–H dissociation bond is $E_b=83.0$ Kcal/mol [16], which is larger than the E_1 and E_2 of DMZn. So the effect of plasma on DMZn molecule is larger than that on H_2S molecule. In the case of ZnS growth with plasma assistance, more DMZn molecules and zinc atoms are absorbed on the film surface than H_2S molecules, which result to zinc rich films. Compared to the growth without plasma assistance, the flow rate of H_2S has to be increased to fabricate ZnS films with stoichiometric ratio in the growth with plasma assistance.

Fig. 5 shows room temperature PL spectra of the ZnS films grown at different substrate temperatures. The VI/II flow proportion was fixed at 14:1. It should be noted that every PL spectrum contains two PL bands except the spectrum of sample grown at 150 °C. The high-energy band at about 340 nm is attributed to near band-edge emission (NBE) [17]. The low-energy band at about 390 nm also appears in the PL spectra of silica substrates without depositing ZnS films, and is absent in the PL spectra of ZnS deposited on sapphire substrate. Therefore, it should be originated from the silica glass substrates, which was discussed usually in some references on silica luminescence [18,19]. Because the S/Zn atomic ratio in the films approaches stoichiometric ratio, the visible emission that is attributed to zinc vacancy luminescence was not observed. All the PL spectra were measured under the same conditions, so the PL relative intensities could be compared with each other. For the film grown at 150 °C, the NBE band was too weak to be

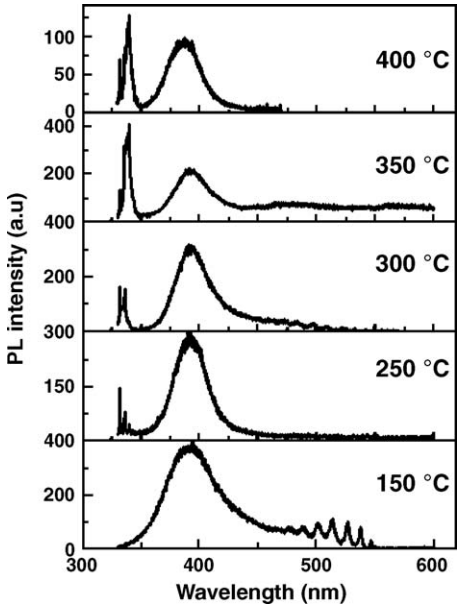

Fig. 5. PL spectra of the ZnS films grown at 150, 250, 300, 350, and 400 °C, respectively.

detected, which may results from lots of defects in the film caused by over low growth temperature. As the crystal quality of ZnS films is improved with increasing growth temperature, the NBE intensity also increases. At 350 °C, the NBE intensity reaches the maximum. When the growth temperature is increased to 400 °C, the NBE intensity shows a certain decrease instead of increase. It indicates the film grown at 350 °C has the highest optical quality, which is in agreement with the XRD result.

4. Conclusion

ZnS thin films with single-phase zinc blende structure were fabricated on silica glass substrates by PA-MOCVD. XRD spectra indicated that the films were single cubic structure when the growth temperature was higher than 150 °C. The optimal growth temperature of ZnS was 350 °C, at which the largest grain size and the strongest NBE were obtained. In the case of ZnS growth with plasma assistance, higher VI/II flow proportions in comparison with that without plasma assistance were required for fabricating stoichiometric films, indicating that the effect of plasma assistance on DMZn is more significant than that on H_2S molecules.

Acknowledgement

This work is supported by the Key Project of National Natural Science Foundation of China under Grant No. 60336020, the National Natural Science Foundation of China under Grant No. 60278031, No. 60376009, No. 60506014, No. 50402016 and No. 60501025, the Innovation Project of Chinese Academy of Sciences.

References

[1] J. Cheon, D.S. Talaga, J.I. Zink, J. Am. Chem. Soc 119 (1997) 163.
[2] A.L. Fahrenbruch, J. Cryst. Growth 39 (1977) 73.
[3] H. Murray, A. Tosser, Thin Solid Films 24 (1974) 165.
[4] M. McLaughlin, H.F. Sakeek, P. Maguire, W.G. Graham, J. Molloy, T. Morrow, S. Laverty, J. Anderson, Appl. Phys. Lett. 63 (1993) 1865.
[5] A. Abounadi, M.D. Blasio, D. Bouchara, J. Calas, M. Averous, O. Briot, N. Briot, T. Cloitre, R.L. Aulombard, Phys. Rev., B 50 (1994) 11677.
[6] S.H. Su, P.R. Tsai, M. Yokoyama, Y.K. Su, J. Electrochem. Soc. 143 (1996) 4116.
[7] H. Kina, Y. Yamada, Y. Maruta, Y. Tamura, J. Cryst. Growth 169 (1996) 33.
[8] M. Migita, O. Kanehisa, M. Shiini, H. Yamamoto, J. Cryst. Growth 93 (1988) 686.
[9] K. Ichino, T. Onishi, Y. Kawakami, S. Fujita, S. Fujita, J. Cryst. Growth 138 (1994) 28.
[10] M. Gunasekaran, R. Gopalakrishnan, P. Ramasamy, Mater. Lett. 58 (2004) 67.
[11] J. Vidal, O. de Melo, O. Vigil, N. Lopez, G. Contreras-Puente, O. Zelaya-Angel, Thin Solid Films 419 (2002) 118.
[12] K. Hirabayashi, O. Kogure, Jpn. J. Appl. Phys. 24 (1985) 1484.
[13] H. Hiramatsu, H. Ohta, M. Hirano, H. Hosono, Solid State Commun. 124 (2002) 411.
[14] W.T. Lim, C.H. Lee, Thin Solid Films 353 (1999) 12.
[15] R.L. Jackson, Chem. Phys. Lett. 163 (1989) 315.
[16] S.R. Gunn, J. Phys. Chem. 68 (1964) 949.
[17] S. Nakamura, T. Sakashita, Y. Yamada, T. Taguchi, J. Cryst. Growth 184/185 (1998) 1110.
[18] B. Bhattacharjee, D. Ganguli, K. Iakoubovskii, A. Stesmans, S. Chaudhuri, Bull. Mater. Sci. 25 (2002) 175.
[19] Y. Sakurai, J. Non-Cryst. Solids 271 (2000) 218.